High Strength Steel Weld Metals - Developments with Ni and Mn

By Keehan, Enda*, Karlsson, Leif**, Murugananth, Marimuthu***, Andrén, Hans-Olof* and Bhadeshia, Harshad***

* Department of Experimental Physics, Chalmers University of Technology, SE - 412 96 Göteborg, Sweden
** ESAB AB, P.O. Box 8004, SE - 402 77 Göteborg, Sweden
*** University of Cambridge, Department of Materials Science and Metallurgy, Pembroke Street, Cambridge CB2 3QZ, U.K.

Abstract

New development routes were explored to increase toughness while maintaining strength in high-strength steel weld metals. An analysis using neural network modelling suggested that impact strength could be increased at moderate expense to yield strength in 7 - 9 wt. % Ni weld metals by reducing manganese concentration. Based on these predictions, shielded metal arc welding was used to prepare weld metals with Ni at 7 and 9 wt. % while Mn was at 2.0 or 0.5 wt. %. Tensile testing showed that these weld metals have yield strengths of 720 - 850 MPa. Charpy toughness levels up to 113 J at -40 °C and 101 J at -60 °C were recorded. Light optical microscopy, scanning and transmission electron microscopy were used to characterise the microstructure and investigate the presence of retained austenite, martensite and bainite. The dramatic synergistic effect of nickel and manganese on microstructure and properties is discussed.

1. Background

Today, as greater expectations are placed on engineering, high-strength steels are increasingly employed. Steels with yield strengths greater than 1000 MPa that possess good toughness at low temperatures have been available for some time. In many applications it is a structural requirement that weld metal with matching or over matching strength is used in the joining of these steels in order to avoid design limitations. It is well known that problems arise in maintaining a high weld metal toughness as yield strength exceeds 690 [1].

Ni and Mn both refine the microstructure and are commonly added to weld metals in order to simultaneously increase strength and toughness. Both also reduce the austenite to ferrite transformation temperature. Additionally, Ni does not form carbides and remains in solution, thereby hardening ferrite [2, 3]. This element also influences the dislocation core structure of ferrite at low temperatures in such a manner that plastic deformation is accommodated [4].

To date, high-strength steel weld metals have usually contained Ni levels less than 4 wt. % and Mn concentrations between 1 and 3 wt. % [1, 5-11]. Results produced using a variety of welding methods, generated yield strengths ranging from below 500 MPa to above 1000 MPa. However, good toughness was mostly achieved at lower yield strengths. For example, Svensson used shielded metal arc welding (SMAW) and a composition of 1.4 wt. % Mn + 0.12 wt. % C to achieve Charpy toughness values of 140 J at - 40 ºC at a yield strength of 520 MPa [10].

In another study, Lord used the composition of a commercial SMAW consumable (ESAB, OK 75.78; 3 Ni, 2 Mn, 0.5 Cr, 0.6 Mo, 0.05 C) as the basis for his development work [12]. Based on the frequent perception that nickel improves the toughness of ferrite [13], Lord increased Ni concentrations from 3 to 4 wt. % at decreasing Mn levels between 1.1 and 0.8

wt. %. In doing so, the toughness increased from 63 to 74 J at -60 ºC but the yield strength was reduced from 837 to 809 MPa. Lord also investigated the effects of other elements such as Cr, but never managed to beat the properties of OK 75.78. Similar development routes with Ni additions and Mn reductions were taken by Kang [14] introducing Ni additions up to 7.45 wt. %. Compositions with high and low levels of Mn (0.40 to 1.76 wt. %) in combination with Ni levels between 1.08 and 7.45 wt. % were investigated. The best toughness (55 J at - 60 ºC) was achieved with high levels of Ni combined with low Mn and a tensile strength of 684 MPa was predicted from hardness measurements. Microstructural analysis confirmed the presence of lath martensite and various forms of ferrite.

2. Neural Network Modelling

With Lord's work [12] as our basis, neural network modelling was engaged to optimise the development process and allow the effects of a wide variety of parameters to be perceived. This method and its advantages are further described in [15-17]. A brief description of the modelling applied in this research is presented here and further details may be found in [18].

Four neural network models were constructed to predict toughness, yield strength (YS), ultimate tensile strength (UTS) and elongation percentage (Elong) based on a database of experimental weld metal results. Since it is frequently found that a committee of models can give better predictions [15, 16], an assessment was made for the optimum size of committee for each mechanical property as described in Table 1.

A contour plot was generated for predicting toughness behaviour at -40 ºC that resulted from variations in manganese and nickel with respect to each other and is shown in Figure 1. The plots display surprising results in that manganese additions in excess of 1 wt. % are predicted to reduce toughness at all nickel concentrations. Additionally they suggest that below a certain critical concentration of manganese, controlled additions of nickel, can lead to an increase in toughness as well as strength, however the reverse mechanical behaviour was predicted if nickel exceeded critical levels dependent on the manganese concentration. These latter predictions contradicted generally held perceptions that nickel additions always lead to toughness increase. Comparisons between model predictions and recorded properties will be made and discussed later.

Model	No. of members in committee	σ_υ (Max. Perceived noise)
Toughness / J	5	0.083
YS / MPa	13	0.040
UTS / MPa	5	0.023
Elong / %	2	0.064

Table 1 Some basic neural network model characteristics.

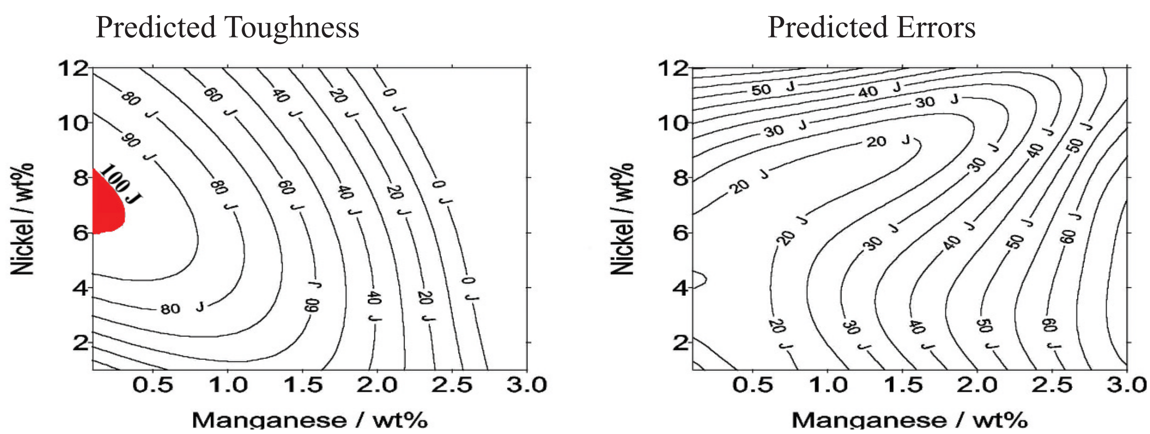

Figure 1 Contour plots showing the calculated weld metal toughness at -40 ºC as a function of manganese and nickel concentration. The predicted errors represent ± 1σ of uncertainty.

3. Experimental Procedures

Based on the neural network estimates five experimental weld metals were produced using SMAW. Welded joints were made according to ISO 2560 using 20 mm plates with a backing plate. The joints were buttered before the deposition of the experimental weld metals that took place in 33 cm runs with three runs per layer. These procedures limited dilution of the weld metal allowing accurate evaluation of the weld metal properties. The welding parameters utilised are presented in Table 2.

Samples of weld metal were analysed using optical emission spectrometry and Leco combustion equipment. The acquired results are also presented in the Table 2.

Charpy impact testing and tensile testing were performed in compliance with standard EN 10045-1. For Charpy testing, transverse specimens were machined having a cross section of 10 × 10 mm. These were then notched perpendicular to the welding direction in the weld metal centre and 2 or 3 specimens were tested at each temperature. Tensile specimens were machined longitudinally from the weld deposits with a specimen diameter of 10 mm and a gauge length of 70 mm.

Weld Metal	Alloy 1	Alloy 2	Alloy 3	Alloy 4	Alloy 5
E / kJ mm-1	1.2	1.2	1.0	1.0	0.7
I. P. T. / °C	250	250	250	200	200
$T_{8/5}$ / s	12	11	10	7	5
C *	0.032	0.031	0.024	0.023	0.026
Si	0.25	0.27	0.35	0.41	0.34
Mn	2.0	2.1	0.6	0.7	0.4
P	0.011	0.011	0.012	0.008	0.007
S*	0.008	0.008	0.008	0.009	0.008
Cr	0.47	0.48	0.21	0.19	0.20
Ni	7.2	9.2	6.6	6.8	8.7
Mo	0.63	0.64	0.40	0.40	0.41
O (ppm)*	380	340	400	360	367
N (ppm)*	250	260	197	105	130

Table 2 Welding parameters and chemical composition. Welding parameters presented are energy input (E), interpass temperature (I.P.T.) and the estimated cooling time between 800 and 500 °C ($T_{8/5}$). Composition is in wt. % unless otherwise stated and '*' indicate elements analysed using Leco Combustion equipment.

Microstructural characterisation was performed with light optical microscopy (LOM) and analytical electron microscopy (SEM & TEM). Specimens from the weld metal cross section, perpendicular to the welding direction were mounted in bakelite for LOM and SEM investigations. These were wet ground and polished to 1 µm before exposing the microstructure with 2 % nital etchant. For TEM investigations, 3 mm disc shape specimens perpendicular to the welding direction were ground to between 50 and 80 µm. The discs were then jet electropolished using 10 % perchloric acid in methanol which was cooled to -35 ºC. Finally, X-ray diffraction was carried out on the last bead of weld Alloys 1, 2 and 3. It was engaged as a complement to electron diffraction to clarify and quantify the presence of retained austenite.

4. Results and Discussion

4.1 Microstructure

Microstructural investigations show the presence of retained austenite, martensite and bainite within these alloys. It was found that interpass temperature, cooling rate and alloying content play crucial roles in microstructural transformations. At low cooling rates, bainite forms while at higher cooling rates martensite forms. Selected microscopy results are presented in Figures 2 to 4. SEM & TEM results show that the general microstructural morphologies of these welds are martensitic / bainitic with films of retained austenite between the plates. The distinction between bainite and martensite is unclear and further work using other experimental techniques are needed to determine the exact nature. Electron diffraction confirmed while X-ray diffraction quantified the presence of the retained austenite in these alloys. The vol. fraction of austenite recorded with X-ray diffraction was 1.5 +/- 0.1 %, 0.8 +/- 0.1 % and 2.2 +/- 0.1 % for Alloys 1, 2 and 3 respectively. The effect of manganese reductions on grain morphology is seen in figure 4 by comparing the microstructure of Alloy 1 (Mn = 2.0 wt. %) with Alloy 3 (Mn = 0.6 wt. %) and the effect of nickel variations is seen by comparing the microstructure of Alloys 1 and 2 (Ni = 7.2 and 9.2 wt. % respectively). As nickel concentration increases, the microstructure changes from coarse to finer grains.

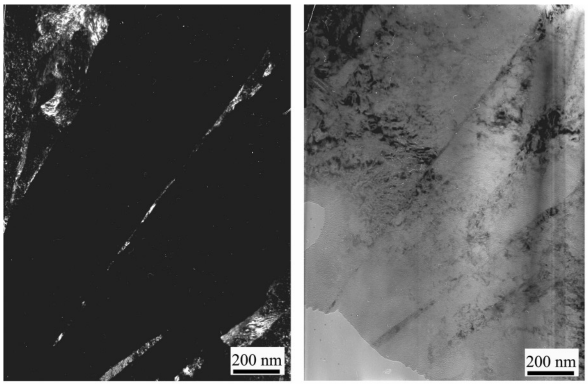

Figure 2 TEM micrographs showing a dark and bright field image of the same area that indicate the presence of austenite thin films in the last bead of Alloy 1.

Figure 3 TEM micrograph of the last bead from Alloy 1 exhibiting a martensitic / bainitic microstructure.

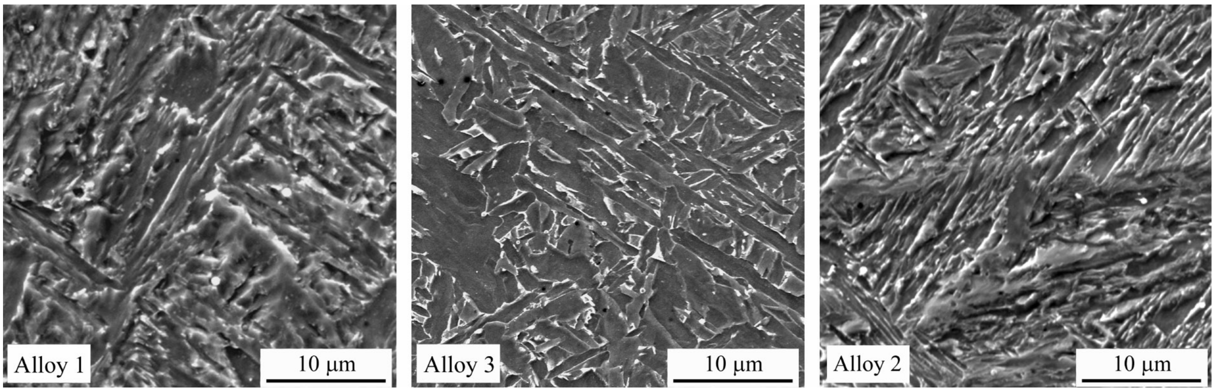

Figure 4 SEM micrographs from the last bead showing the microstructural effects of manganese reductions from 2.0 wt. % in Alloy 1 to 0.6 wt.% in Alloy 3. Comparing the microstructure of Alloy 1 with Alloy 2 shows the microstructural effects of increased nickel concentrations from 7.2 to 9.2 wt.%.

4.2 Mechanical Properties

The recorded mechanical properties of the weld alloys are presented both in Table 3 and Figure 5. Predicted properties from the neural network models for the exact compositions and welding parameters utilized are also presented in Table 3 to allow easy comparisons. The results are exciting since all yield strengths recorded lie over 720 MPa and toughness levels reach 113 J at -40 °C.

When comparisons are made in tensile properties, Alloys 1 and 2, with similar high levels of manganese (≈ 2 wt. %) and varied nickel (≈ 7 and 9 wt. %) achieved yield strengths of 795 and 848 MPa respectively. The UTS of both these alloys is also very high with both greater than 1000 MPa. The difference between yield strength and UTS in both cases is large with the ratio of YS / UTS below the common maximum requirements of 0.85 or 0.9. When the Charpy impact results are analysed, these weld metals exhibited the poorest toughness levels with values of 32 and 12 J at -40 °C. As expected from neural network predictions (Figure 1) Alloy 1 achieved the better toughness with its lower nickel content.

Comparing mechanical properties of Alloys 1 and 3 shows the effect of reducing manganese concentration. A clear drop in yield strength is experienced, with Alloy 3 dropping 75 MPa to 721 MPa. However toughness dramatically increases at these reduced Mn levels to 113 J at -40 °C. These results confirm neural network toughness predictions that Mn reductions at these Ni levels increase toughness. The role of interpass temperature is considered by taking Alloys 3 and 4 into account. By decreasing interpass temperature to 200 °C from 250 ºC, strength goes up from 721 MPa to 816 MPa at moderate expense to toughness.

The role of nickel is investigated with low Mn levels in Alloys 4 and 5. An interpass temperature of 200 °C was also chosen for Alloy 5 with the aim of having good strength while still maintaining toughness. Both these alloys display good strength levels with 816 and 827 MPa recorded. Interestingly the difference between YS and UTS is much less than previously seen with Alloys 1 and 2. Toughness drops with higher Ni concentration and again confirms neural network predictions that Ni must be added in a controlled manner. Tensile properties are also in very good agreement with neural network predictions.

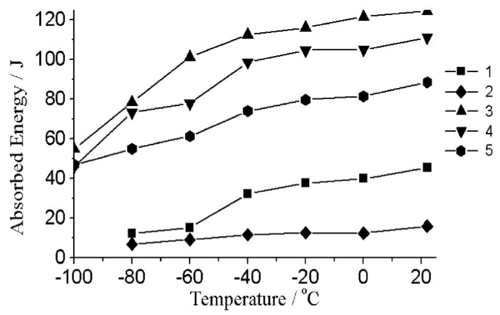

Figure 5 The mean Charpy impact toughness at each temperature for weld Alloys 1-5.

Overall, there is fair agreement between predicted and recorded values for the mechanical properties of the weld alloys, which thus validate the models. The models correctly predicted both the UTS and Elong within error for all the alloys, while three alloys were correctly predicted within error for the YS.

Weld Metal		Alloy 1	Alloy 2	Alloy 3	Alloy 4	Alloy 5
YS / MPa	(Recorded)	795	848	721	816	827
	(Predicted)	833 ± 27	838 ± 26	754 ± 21	804 ± 21	827 ± 36
UTS / MPa	(Recorded)	1006	1051	823	850	895
	(Predicted)	999 ± 16	1052 ± 12	833 ± 11	857 ± 9	904 ± 18
YS / UTS	(Recorded)	0.79	0.81	0.88	0.96	0.93
Elong. / %	(Recorded)	15	13	21	19	18
	(Predicted)	14.8 ±1	12.1 ±1	20.9 ± 1	19.7 ± 1	17.6 ± 1

Table 3. Recorded and predicted mechanical properties for the exact compositions and welding parameters of Alloys 1 - 5.

4.3 Influence of Ni and Mn

Ni and Mn have effects dependant on each other that are still not fully understood on a microstructural level and further work is needed to characterise their relationship. Once Ni exceeds a critical point, which depends on Mn concentration, toughness decreases. Up to this critical point it is thought that nickel additions cause toughness increase by increasing the number of grain boundaries, through grain refinement and by influencing the dislocation core structure.

Further work is necessary with techniques such as energy filtered transmission electron microscopy and atom probe field ion microscopy to clarify the effect of nickel and manganese. With these techniques it is possible to map the elemental distribution on a very fine scale and make correlations with both the microstructure and mechanical properties. On completion of this work, an increased understanding will be attained as to why nickel must be added in a controlled manner with respect to manganese and routes that may lead to further increases in toughness and strength will be visible.

5. Conclusions

Neural network simulations indicated that above manganese levels of 2 wt. % nickel additions were predicted to cause a decrease in toughness and below 2 wt. % care must be taken not to exceed critical levels of Ni. Based on these predictions experimental weld metals were produced with Mn levels at 0.5 or 2 wt. % and Ni levels at 7 or 9 wt. %.

Microstructural investigations concluded a martensitic / bainitic microstructure with films of retained austenite in these alloys. The distinction between martensite and bainite was difficult and further work is needed. Nickel additions lead to grain refinement within the microstructure.

The variation of nickel and manganese has dramatic effects on the mechanical properties. The greatest toughness levels recorded (113 J at -40 ^{O}C) were with Mn levels less than 0.7 wt. % and at Ni levels of approximately 7 wt. %. These compositions recorded yield strengths greater than 800 MPa with an interpass temperature of 200 ^{O}C and high cooling rates. At Mn levels greater than 2 wt. % yield strength reached 848 MPa however toughness dramatically decreased to less than 20 J at - 60 ^{O}C.

The four neural network models applied were proved reliable and correctly estimated the mechanical behaviour for varied nickel and manganese compositions.

6. Acknowledgements

ESAB AB is thanked for the production of experimental weld metals, permission to publish results and financial support. KK-stiftelsen of Sweden is thanked for additional financial support.

References

1) L.-E. Svensson: Svetsaren, **54**, January (1999).
2) A.C. Davies: Welding Science and Technology. 10 Ed. The Science & Practice of Welding. Vol. **1**. (1992): Cambridge University Press.
3) ASM: Properties and Selection Iron, Steel and High Performance Alloys. 10 Ed. ASM Handbook. Vol. **1** (1990).
4) L.-E. Svensson: Control of mircostructure and properties in steel arc welds, CRC Press, Inc (1994) p 69
5) J.F. Deloach: Proceedings, International Conference on Welding Technology, Material and Fracture, (1990), Geesthacht, Germany: Gournay-sur-Marne, France; IITT International; 1990.
6) P.R. Oldland, C.W. Ramsay, D.K. Matlock, D.L. Olson: Welding Journal, **68**, April, (1989), p. 158.
7) M.G. Vassilaros, E.J. Czyryca: Proceedings, Advances in Low-Carbon High Strength Ferrous Alloys (LCFA-92), Jamshedpur (India), March 25-28, (1992): Key Engineering Materials (Switzerland).
8) D.B. Fleming, A.Q. Bracarense, S. Liu, D.L. Olson: Welding Journal (USA), **75** June (1996), p. 171.
9) D.E. McRobie, J.F. Knott, Material Science and Technology, **1** May (1985), p. 357.
10) L.-E. Svensson, B. Gretoft: Welding Journal, **69** December (1990), p. 454.
11) T.W. Lau, M.M. Sadowsky, T.H. North, G.C. Weaterly: The Metallurgical Society / AIME, 1987 p. 349.
12) M. Lord: Design and Modelling of Ultra - High Strength Steel Weld Deposits, Ph. D. Thesis, (1999), University of Cambridge: Cambridge.
13) W.C. Leslie: The physical metallurgy of steels. (1981), London: McGraw - Hill.
14) Y. Kang, H.J. Kim, and S.K. Hwang: ISIJ International (Japan), **40** December (2000), p. 1237.
15) D.J.C. Mackay: Neural Computation. (1992), p. 448.
16) D.J.C. Mackay: Neural Computation. (1992), p. 415.
17) H.K.D.H. Bhadeshia: ISIJ International (Japan), **39** October (1999), p. 966.
18) M. Murugananth, H.K.D.H. Bhadeshia, E. Keehan, H.-O. Andrén, L. Karlsson: Proc. 6th Int. Seminar, "Numerical Analysis of Weldability", Oct 1-3 (2001), Graz, Austria.